

UWB LOCALIZATION-OF-THINGS VIA SOFT INFORMATION: NETWORK EXPERIMENTATION IN INDOOR ENVIRONMENT

Carlos A. Gómez-Vega*, Moe Z. Win† and Andrea Conti*

*DE and CNIT, University of Ferrara, email: cgomez@ieee.org, a.conti@ieee.org

†LIDS, Massachusetts Institute of Technology, email: moewin@mit.edu

(Invited Paper)

ABSTRACT

Location awareness is crucial for numerous applications in fifth generation (5G) and beyond ecosystems. Localization-of-things (LoT) via soft information (SI) enables accurate localization, tracking, and navigation of networked nodes. This paper demonstrates real-time SI-based LoT using ultra-wideband (UWB) radios. We consider two data collection approaches and evaluate them via network experimentation in an indoor environment. Experimental results show the potential of SI-based LoT using UWB technology to satisfy service level requirements of 5G and beyond ecosystems.

Index Terms— Localization-of-things, soft information, machine learning, UWB, experimentation.

1. INTRODUCTION

Location awareness [1] is crucial for numerous applications in fifth generation (5G) and beyond ecosystems [2–4] including autonomy [5], smart environments [6], and the Internet-of-Things [7]. The recently proposed soft information (SI) approach enables accurate localization-of-things (LoT) [8]. In particular, LoT requires adequate acquisition and exploitation of SI from measurements and contextual data. This calls for experimental efforts focused on data collection for learning SI from measurements.

Location-aware networks consist of anchors with known positions and agents with unknown positions. To obtain position information, agents perform inter- and intra-node measurements. Inter- and intra-node measurements can be obtained via radio signals [9] and inertial sensors [10], respectively. Specifically, ultra-wideband (UWB) signals [11, 12] are well-suited for inter-node measurements because of their fine delay resolution and robustness to complex wireless environments [11–15]. Owing to its precise positioning capabilities and recent penetration in the market of consumer devices,

The fundamental research described in this paper was supported, in part, by the Office of Naval Research under Grant N62909-22-1-2009 and, in part, by the National Science Foundation under Grant CNS-2148251.

UWB technology has been considered for providing high-accuracy localization in 5G and beyond ecosystems [16].

Existing localization algorithms infer the positions of agents via hard-decision techniques based on single-value estimates (SVEs) such as range estimates from inter-node measurements. The performance of such algorithms degrades in complex wireless environments due to biases caused by multipath propagation and non-line-of-sight (NLOS) conditions. In this regard, machine learning methods have been employed to identify the propagation conditions and mitigate their effects in SVEs [17–19]. In particular, SI-based localization considers the relationships between measurements and position information in a probabilistic approach [8, 20]. Such relationships are encapsulated by generative models that can be learned from measurements and allow soft-decision localization based on the odds of all the possible position features.

A fundamental aspect for unleashing the capabilities of SI-based LoT is how to collect measurements for learning SI. In particular, a well-designed data collection methodology will enable learning reliable generative models for high-accuracy SI-based LoT. The goal of this paper is to demonstrate real-time SI-based LoT under different data collection approaches using off-the-shelf UWB radios. The key idea consists of performing network experimentation [21] to collect measurements for learning SI.

This paper demonstrates real-time SI-based UWB LoT under two different data collection approaches via network experimentation in an indoor environment. The key contributions of this paper are as follows:

- demonstration of real-time SI-based UWB LoT via network experimentation in an indoor environment; and
- quantification of the performance provided by generative models under different data collection approaches.

The remaining sections are organized as follows: Section 2 presents an overview of SI-based LoT. Section 3 describes the network experiments. Section 4 presents the experimental results. Finally, Section 5 gives our conclusions.

Notations: Random variables (RVs) are displayed in sans serif, upright fonts; their realizations in serif, italic fonts. Vectors are denoted by bold lowercase letters. For example, a variable is denoted by x ; and a random vector and its realization are denoted by \mathbf{x} and \boldsymbol{x} , respectively. Sets are denoted by calligraphic font. For example, a set is denoted by \mathcal{X} . The function $f_{\mathbf{x}}(\boldsymbol{x})$ denotes the probability distribution function (PDF) of a RV \mathbf{x} ; and $f_{\mathbf{x}|\mathbf{y}}(\boldsymbol{x}|\boldsymbol{y})$ denotes the PDF of \mathbf{x} conditioned on $\mathbf{y} = \boldsymbol{y}$. Operators $\mathbb{E}\{\cdot\}$ and $\mathbb{P}\{\cdot\}$ denote the expectation and probability of the argument. The norm of a vector \boldsymbol{x} is denoted by $\|\boldsymbol{x}\|$.

2. PRELIMINARIES

This section presents an overview of SI-based LoT focused on the setting that will be evaluated via experimentation.

2.1. System Model

Consider a non-cooperative location-aware network consisting of N_b anchors and a single agent. The index set of anchors is denoted by $\mathcal{N}_b = \{1, 2, \dots, N_b\}$. The positions of the agent and anchor i are denoted by \boldsymbol{p} and \boldsymbol{p}_i , respectively. The distance between the agent and anchor i is denoted by $d_i = \|\boldsymbol{p} - \boldsymbol{p}_i\|$. The goal is to determine the agent position based on inter-node measurements and environmental information. Let \boldsymbol{y}_i denote the inter-node measurements that the agent obtains from anchor i . The measurements in \boldsymbol{y}_i are related to a feature vector $\boldsymbol{\theta}_i$ that depends on \boldsymbol{p} . In particular, we consider range measurements $\boldsymbol{y}_i = [\hat{d}_i]$ and features $\boldsymbol{\theta}_i = [d_i]$. Furthermore, let $\boldsymbol{\mu}$ denote the environmental information. Such information provides prior knowledge for the inference of \boldsymbol{p} . Specifically, we consider the context provided by a digital map.

2.2. SI-based LoT

SI-based LoT exploits soft feature information (SFI) and soft context information (SCI) to infer the positions of agents [8]. Specifically, SFI and SCI encapsulate the position information provided by measurements and the environmental information provided by contextual data, respectively.

In a non-Bayesian setting, the positions and features are unknown parameters. In this setting, the SFI provided by a measurement \boldsymbol{y} is a function of the feature vector $\boldsymbol{\theta}$ given by

$$\mathcal{L}_{\boldsymbol{y}}(\boldsymbol{\theta}) \propto f_{\boldsymbol{y}}(\boldsymbol{y}; \boldsymbol{\theta}). \quad (1)$$

In a Bayesian setting, the positions and features are considered as RVs and the SFI is given by

$$\mathcal{L}_{\boldsymbol{y}}(\boldsymbol{\theta}) \propto f_{\boldsymbol{y}|\boldsymbol{\theta}}(\boldsymbol{y}|\boldsymbol{\theta}). \quad (2)$$

In particular, we consider soft range information (SRI) obtained from range measurements, i.e., $\mathcal{L}_d(d)$.

The SCI provided by contextual data is a function of the feature vector $\boldsymbol{\theta}$. In a Bayesian setting, the SCI provided by a digital map can be incorporated as a prior distribution of the agent position. Hence, the SCI provided by $\boldsymbol{\mu}$ is given as

$$\Phi_{\boldsymbol{\mu}}(\boldsymbol{p}) \propto f_{\boldsymbol{p}}(\boldsymbol{p}; \boldsymbol{\mu}). \quad (3)$$

In non-cooperative localization, the position of the agent is inferred based on the measurements and contextual data obtained. In a non-Bayesian setting, the position estimate is given by

$$\hat{\boldsymbol{p}} = \arg \max_{\boldsymbol{p}} \prod_{i \in \mathcal{N}_b} \mathcal{L}_{\hat{d}_i}(\tilde{d}_i). \quad (4)$$

where $\tilde{d}_i = \|\tilde{\boldsymbol{p}} - \boldsymbol{p}_i\|$. In contrast to (4), SCI can be incorporated directly in a Bayesian setting. Considering the SCI, the position estimate is given by

$$\hat{\boldsymbol{p}} = \arg \max_{\boldsymbol{p}} \Phi_{\boldsymbol{\mu}}(\tilde{\boldsymbol{p}}) \prod_{i \in \mathcal{N}_b} \mathcal{L}_{\hat{d}_i}(\tilde{d}_i). \quad (5)$$

2.3. Acquisition and Exploitation of SI for LoT

SI-based LoT consists of three steps: (i) acquisition of measurements and contextual data; (ii) characterization of SFI and SCI; and (iii) position inference based on SFI and SCI [8]. The SFI can be characterized by a generative model [8, 20]. Such a model can be obtained from measurements and position features via machine learning techniques [22]. The SFI of a new measurement \boldsymbol{y} is obtained from the generative model for $\mathcal{L}_{\boldsymbol{y}}(\boldsymbol{\theta})$. SI-based algorithms for LoT are divided in two phases, namely offline training and online operation [8]. In the training phase, a generative model is learned from measurements, position features, and contextual data. In the operation phase, the SI of new measurements and contextual data is determined from the generative model to infer the positions of agents. The training phase is performed offline since it requires acquiring measurements and learning SI from them. The operation phase is performed online since it determines the SI of new measurements to infer the positions of agents.

The characterization of SFI from measurements can be challenging, especially for complex wireless environments. Machine learning techniques to learn generative models for SFI include fitting Gaussian mixture models [8], kernel density estimation [20], and deep neural networks [23]. While the SI framework can be applied using any kind of measurements and features, the methodology and techniques to learn and exploit SI are technology-dependent. For example, pre-processing techniques may be required to facilitate training. Moreover, the obtained measurements can have high dimensionality, e.g., vectors with samples of the received waveform. In such a case, dimensionality reduction is crucial for efficient LoT [8].



Fig. 1. Experimentation environment at the Department of Engineering, University of Ferrara.

3. NETWORK EXPERIMENTATION

This section describes the network experiments for collecting measurements to learn SI and evaluate SI-based LoT.

3.1. Measurement Setup

Consider a location-aware network with N_b anchors and a single agent. The anchor deployment is fixed and N_l landmark positions with index set $\mathcal{N}_l = \{1, 2, \dots, N_l\}$ are considered. Specifically, the considered LoT system consists of UWB radios providing only range measurements. The UWB radios employed in the experimentation are compliant with the IEEE 802.15.4 standard. Such radios operate at 3.9 GHz with 500 MHz bandwidth, and provide a range measurement via a proprietary two-way ranging technique every 100 ms.

The network experiments are performed in a typical indoor environment at the Department of Engineering, University of Ferrara (see Fig. 1). The experimental setup consists of $N_b = 3$ anchors (labeled B1-B3) and $N_l = 51$ landmarks. Fig. 2 shows the map of the experimentation environment with the positions of anchors and landmarks. The choice of the anchor deployment is to have at least one anchor in NLOS conditions for most landmark positions. This choice is made to demonstrate SI-based localization techniques in a challenging scenario where conventional methods typically fail to provide desirable performance.

3.2. Measurement Campaign

Network experiments for acquiring measurements to learn SI can be performed under two different approaches. The first approach consists of collecting measurements to provide a general description of SFI for operating in environments similar to the experimentation environment but not necessarily the same [8, 20]. Examples of network experiments for this purpose include those involving two nodes in line-of-sight (LOS) conditions with different types of clutter and NLOS conditions with different types of blockages at different separation distances (e.g., see [21]). In contrast, the second approach

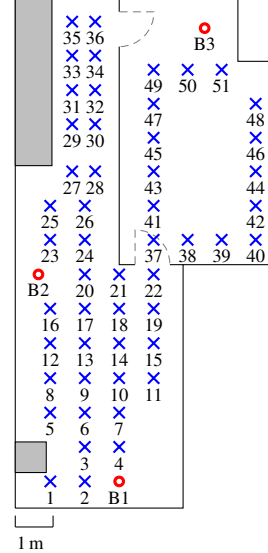


Fig. 2. Map of the experimentation environment with the positions of anchors (red annulus) and landmarks (blue crosses). The grey areas represent locations that cannot be accessed by the nodes.

consists of collecting measurements to provide a specific description of SFI for operating in the same environment. In this approach, the goal is to collect measurements for characterizing the SFI provided by each anchor in a fixed position. While the first approach enables accurate localization by learning a single general model for any anchor operating in similar environments, the latter can provide enhanced localization performance in the specific environment by learning a model for each deployed anchor. In the following, we refer to these approaches as general and site-specific, respectively.

The characterization of the SFI provided by an anchor requires measurements with the agent placed in different positions. First, we collect measurements between an anchor and an agent in general settings considering both LOS and NLOS conditions for distances ranging from 0.3 to 15 m. The experiments for LOS conditions are performed in the two areas of the experimentation environment, namely the corridor and the meeting room (see Fig. 1). The experiments for NLOS are performed between the two areas with walls and doors as blockages considering different angles among the nodes. In the site-specific setting, the range measurements are collected for the three anchors in Fig. 2 with the agent placed in all the considered landmarks. The experiments in both settings consist of placing the agent in the corresponding position with the antenna pointing to four predefined directions. To provide further robustness to the wireless environment, two types of experimental conditions are considered: (i) static environment, where the channel conditions are determined by the walls and clutter (chairs and tables), and (ii) dynamic environment, where the channel conditions are changed over time by a person walking in the experimentation environment.

Table 1. Performance of localization methods with general and site-specific models. Localization error evaluated in cm.

Method	e_{med}	e_{95}	$P_o(10)$	$P_o(50)$	$P_o(100)$
G1	37.5	162.6	83.5%	37.7%	15.0%
G2	41.6	154.0	85.2%	42.9%	16.3%
G4	34.1	174.7	85.94%	35.13%	15.0%
S1	31.5	105.6	93.3%	19.6%	6.5%
S2	14.8	135.2	63.8%	16.3%	7.3%
S4	14.7	129.1	62.6%	13.6%	6.7%
S1 + SCI	31.5	101.6	93.3%	19.6%	5.3%
S2 + SCI	14.6	102.4	63.5%	15.2%	5.5%
S4 + SCI	14.5	107.5	62.4%	12.7%	5.5%

4. EXPERIMENTAL RESULTS

This section evaluates real-time SI-based LoT under the two data collection approaches considered.

4.1. Performance Metrics

Consider the localization error and localization error outage (LEO) as the performance metrics for the evaluation of SI-based LoT [21]. Specifically, the localization error for an agent placed at \mathbf{p} is given by

$$e(\mathbf{p}) = \|\hat{\mathbf{p}} - \mathbf{p}\|. \quad (6)$$

The LEO is given in terms of the outage probability based on the localization error as

$$P_o(e_{\text{th}}) = \mathbb{P}\{e(\mathbf{p}) > e_{\text{th}}\} = \mathbb{E}\{\mathbb{1}_{(e_{\text{th}}, \infty)}(e(\mathbf{p}))\} \quad (7)$$

where e_{th} is the target error and $\mathbb{1}_{\mathcal{A}}(x) = 1$ when $x \in \mathcal{A}$ and 0 otherwise. We consider the median and 95th percentile of the localization error, which are given in terms of the LEO as $e_{\text{med}} = P_o^{-1}(0.5)$ and $e_{95} = P_o^{-1}(0.05)$, respectively.

4.2. Performance of SI-based LoT

The localization performance is evaluated for different generative models learned from the collected measurements. We consider learning SRI by fitting training measurements to Gaussian mixture models with different number of components, namely 1, 2, and 4. The measurements of the general setting are all employed for training. The measurements of the site-specific setting are separated for training (70%) and performance evaluation (30%). The localization methods using SRI learned from measurements for general and site-specific settings are denoted as G_i and S_i , where i indicates the number of components in the Gaussian mixture models. We evaluate the performance provided by the generative models on the test data obtained in the site-specific setting. The performance is also evaluated considering SCI provided by a digital map of the experimentation environment. Specifically, the SCI is modeled as a uniform distribution over the set of allowed positions (i.e., the white area in Fig. 2).

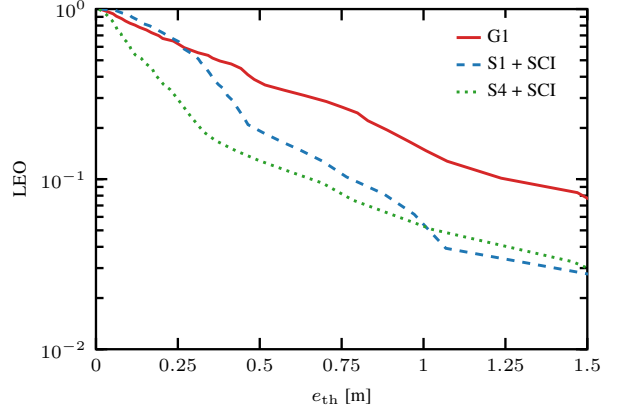


Fig. 3. LEO for localization methods with general and site-specific models.

Table 1 shows the performance of different localization methods with general and site-specific models on validation data. We observe that the generative models learned from site-specific measurements provide higher localization accuracy. For example, the localization method S2 reduces the median localization error with respect to G2 by 64%. Furthermore, SCI provides a further performance improvement by adding map information. Note that methods using site-specific models in combination with SCI can provide submeter accuracy for 94% of the cases. In addition, these techniques can achieve a localization accuracy below 10 cm for at most 37% of the cases. To provide a further comparison, Fig. 3 shows the LEO for different localization techniques on validation data, where we observe the gain provided by training with site-specific measurements over the case with those in a general setting. While a site-specific data collection can improve localization accuracy, it requires a training phase with higher complexity, i.e., measurements with all the deployed anchors. Therefore, there is a tradeoff between the complexity of the training phase and the localization performance. In the deployed LoT system with the developed models, the position estimate is updated before new measurements are available, confirming real-time operation.

5. CONCLUSION

This paper demonstrates real-time SI-based UWB LoT under two different data collection approaches. We performed network experimentation to collect measurements for learning SI and evaluating SI-based LoT. Experimental results show that SI-based techniques using only range measurements can provide desirable localization performance, especially with generative models learned from site-specific measurements. In particular, the results reveal a tradeoff between the complexity of the training phase and localization performance. This experimental work shows the potential of SI-based LoT using UWB technology to satisfy service level requirements of 5G and beyond ecosystems.

6. REFERENCES

- [1] M. Z. Win, A. Conti, S. Mazuelas, Y. Shen, W. M. Gifford, D. Dardari, and M. Chiani, “Network localization and navigation via cooperation,” *IEEE Commun. Mag.*, vol. 49, no. 5, pp. 56–62, May 2011.
- [2] *Technical Specification Group Services and System Aspects; Service requirements for the 5G system; Stage 1*, 3rd Generation Partnership Project 3GPP™ TS 22.261 V18.3.0 (2021-06), Jun. 2021, Release 18.
- [3] *Technical Specification Group Services and System Aspects; Study on positioning use cases; Stage 1*, 3rd Generation Partnership Project 3GPP™ TR 22.872 V16.1.0 (2018-09), Sep. 2018, Release 16.
- [4] A. Conti, F. Morselli, Z. Liu, S. Bartoletti, S. Mazuelas, W. C. Lindsey, and M. Z. Win, “Location awareness in beyond 5G networks,” *IEEE Commun. Mag.*, vol. 59, no. 11, pp. 22–27, Nov. 2021, special issue on *Location Awareness for 5G and Beyond*.
- [5] A. Guerra, F. Guidi, D. Dardari, and P. M. Djurić, “Networks of UAVs of low complexity for time-critical localization,” *IEEE Aerosp. Electron. Syst. Mag.*, vol. 37, no. 10, pp. 22–38, Oct. 2022.
- [6] G. Pasolini, C. Buratti, L. Feltrin, F. Zabini, C. De Castro, R. Verdone, and O. Andrisano, “Smart city pilot projects using LoRa and IEEE 802.15.4 technologies,” *MDPI Sensors*, vol. 18, no. 4, Apr. 2018.
- [7] D. Zhang, L. T. Yang, M. Chen, S. Zhao, M. Guo, and Y. Zhang, “Real-time locating systems using active RFID for Internet of Things,” *IEEE Syst. J.*, vol. 10, no. 3, pp. 1226–1235, Sep. 2016.
- [8] A. Conti, S. Mazuelas, S. Bartoletti, W. C. Lindsey, and M. Z. Win, “Soft information for localization-of-things,” *Proc. IEEE*, vol. 107, no. 11, pp. 2240–2264, Nov. 2019.
- [9] F. Gustafsson and F. Gunnarsson, “Mobile positioning using wireless networks: possibilities and fundamental limitations based on available wireless network measurements,” *IEEE Signal Process. Mag.*, vol. 22, no. 4, pp. 41–53, Jul. 2005.
- [10] R. Harle, “A survey of indoor inertial positioning systems for pedestrians,” *IEEE Commun. Surveys Tuts.*, vol. 15, no. 3, pp. 1281–1293, third quarter 2013.
- [11] M. Z. Win and R. A. Scholtz, “Impulse radio: How it works,” *IEEE Commun. Lett.*, vol. 2, no. 2, pp. 36–38, Feb. 1998.
- [12] M. Z. Win and R. A. Scholtz, “On the energy capture of ultra-wide bandwidth signals in dense multipath environments,” *IEEE Commun. Lett.*, vol. 2, no. 9, pp. 245–247, Sep. 1998.
- [13] D. Dardari, A. Conti, U. J. Ferner, A. Giorgetti, and M. Z. Win, “Ranging with ultrawide bandwidth signals in multipath environments,” *Proc. IEEE*, vol. 97, no. 2, pp. 404–426, Feb. 2009, special issue on *Ultra-Wide Bandwidth (UWB) Technology & Emerging Applications*.
- [14] S. Gezici, Z. Tian, G. B. Giannakis, H. Kobayashi, A. F. Molisch, H. V. Poor, and Z. Sahinoglu, “Localization via ultra-wideband radios: A look at positioning aspects for future sensor networks,” *IEEE Signal Process. Mag.*, vol. 22, no. 4, pp. 70–84, Jul. 2005.
- [15] S. Bartoletti, W. Dai, A. Conti, and M. Z. Win, “A mathematical model for wideband ranging,” *IEEE J. Sel. Topics Signal Process.*, vol. 9, no. 2, pp. 216–228, Mar. 2015.
- [16] 5G-PPP Architecture Working Group, *View on 5G Architecture*. The 5G Infrastructure Public Private Partnership, Aug. 2021, version 4.0.
- [17] Y. Zhu, W. Xia, F. Yan, and L. Shen, “NLOS identification via AdaBoost for wireless network localization,” *IEEE Commun. Lett.*, vol. 23, no. 12, pp. 2234–2237, Dec. 2019.
- [18] S. Maranò, W. M. Gifford, H. Wymeersch, and M. Z. Win, “NLOS identification and mitigation for localization based on UWB experimental data,” *IEEE J. Sel. Areas Commun.*, vol. 28, no. 7, pp. 1026–1035, Sep. 2010.
- [19] K. Bregar and M. Mohorčič, “Improving indoor localization using convolutional neural networks on computationally restricted devices,” *IEEE Access*, vol. 6, pp. 17429–17441, 2018.
- [20] S. Mazuelas, A. Conti, J. C. Allen, and M. Z. Win, “Soft range information for network localization,” *IEEE Trans. Signal Process.*, vol. 66, no. 12, pp. 3155–3168, Jun. 2018.
- [21] A. Conti, M. Guerra, D. Dardari, N. Decarli, and M. Z. Win, “Network experimentation for cooperative localization,” *IEEE J. Sel. Areas Commun.*, vol. 30, no. 2, pp. 467–475, Feb. 2012.
- [22] C. M. Bishop, *Pattern Recognition and Machine Learning*. New York, NY, USA: Springer, 2006.
- [23] Y. Li, S. Mazuelas, and Y. Shen, “A deep learning approach for generating soft range information from RF data,” in *IEEE Globecom Workshops*, Madrid, Spain, Dec. 2021, pp. 1–5.